

PLATE FLATNESS METER BASED ON MOIRE FRINGES

Jiro Matsuo Toshiyuki Matsumi Kouichi Kitamura
 Nippon Steel Corporation
 Nagoya works Electronics R & D Laboratories

5-3, Tokai-machi, Tokai-shi
 Aichi-ken, 476, Japan

1618, Ida, Nakahara-ku, Kawasaki-shi
 Kanagawa-ken, 211, Japan

1. ABSTRACT

A plate flatness meter based on the laser moire method was developed. A large grating is installed above a plate transfer line, a laser beam is directed through a concave lens onto the plate on the transfer line. Moire fringes that conform to the surface profile of the plate are formed on the plate. The flatness of the plate as it is transferred can be measured to a high accuracy of $\pm 1.0\text{mm}(2\sigma)$.

2. BACKGROUND

In recent years, increasingly severe flatness requirements have been demanded of plates in view of elimination of leveling work for cost reduction and of introduction of automatic welding machines at the end users. For example, some bridge girder plates must meet wave height requirements of 2 mm or less over the entire length of 1500 mm.

No flatness meters are commercially available that can measure the flatness of plates to such a high degree of accuracy. To determine their flatness to such close tolerances, plates must be examined by inspectors with straightedges. Under this method, the inspector stops the plate and measures the entire surface of the plate with straightedge, expending much time and labor. In view of the available production capacity, there is a limit to the quality assurance of plates by this inspection method.

Given the urgent need for high-accuracy in-line flatness meter. We tackled the development of a plate flatness meter based on the laser moire method.

3. PRINCIPLE

3.1 Principle of moire topography

The principle of moire topography is illustrated in Fig.1. When the object to be measured is viewed from the observation point E, the surface of

the object appears bright where radial rays in a group with S as the center (transmitted light) intersect with radial rays in another group with E as the center (reflected light). As evident from Fig. 1, these intersections are formed as equal distances from the grating surface. Since the grating pitch P is small in reality, the intersections appear continuous laterally and look bright in the sections $Z = Z_1, Z_2, \dots$ in the object and look dark in the intermediate portions. Namely, contour-lines are obtained.

N in Fig. 1 is referred to as the fringe order of the sequence of the light section in question from the grating surface. The depth Z_n for the fringe order $N = n$ and the contour line resolution ΔZ_n are given by

$$Z_n = P\ell n / (d - nP) \quad (1)$$

$$\Delta Z_n = P(Z_n + \ell)^2 / d\ell \quad (2)$$

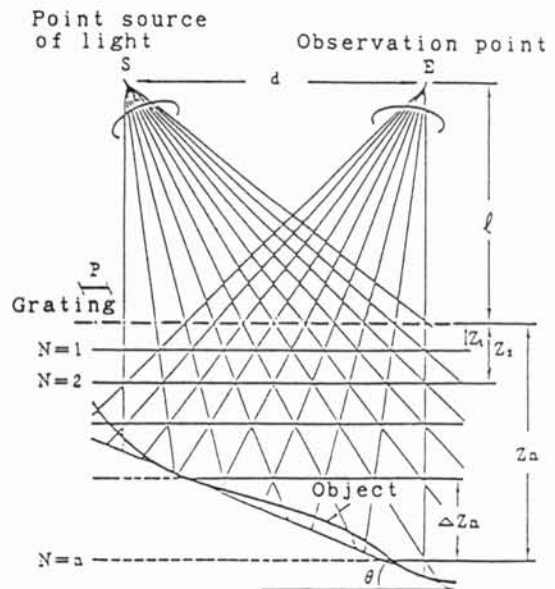


Fig. 1. Principle of moire topography.

In moire topography, contour lines are revealed on the surface of the object to be measured, so that the relative elevation of the contour lines, that is, the surface irregularities of the object, are not known. Various methods are thus devised for knowing the surface irregularities of the object. The plate flatness meter has the method of uniquely assigning the fringe orders (relative fringe orders, to be more exact), regardless of the surface irregularity judgment involved, by setting the relative angle between the transfer roll plane and the light sections larger than the maximum angle of inclination of plate shape. This method is simply called the incline moire method hereinafter.

3.2 Configuration of plate flatness metered system

The configuration of the plate flatness meter system is shown in Fig. 2. To provide distance (lift-off) of at least 500 mm between the grating surface and transfer roll surface for collision avoidance, a highly directional laser was employed

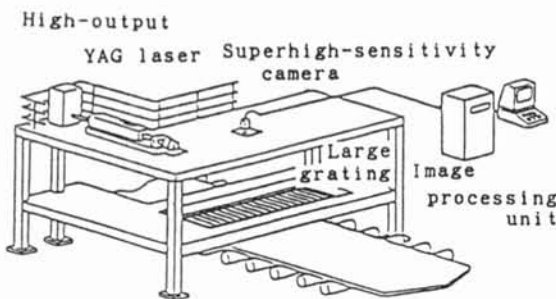


Fig. 2. Configuration of plate flatness meter system.

as the source of light. The laser beam is directed onto the large grating through a beam expander and concave lens.

The main specifications of the optical system are given in Table 1.

An original image of moire fringes formed on a 2,400 mm wide plate with surface waves of approximately 2 mm height is shown in Fig. 3. The image is composed of 512 x 512 x 8 bits.

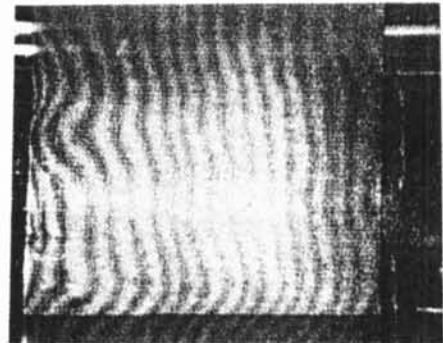


Fig. 3. Original image of moire fringes

4. IMAGE PROCESSING

4.1 Image processing system

The hardware configuration of the image processing system is shown in Fig. 4. Video signals and laser oscillation synchronizing signals are sent to the image processing unit. Smoothing, affine transformation and other preliminary processing are performed in the image processing unit, and image recognition and shape reconstruction are carried out by a 32-bit general-purpose minicomputer.

Table 1. Main specifications of optical system.

Classification	Item	Specification of performance
Large grating	Effective area	5 m (transverse direction) x 2 m (longitudinal direction)
	Grating pitch	1.5 mm
	Tension mechanism	Tension mechanism using Ni-Ti shape memory alloy
Light source	Type	YAG laser (Q-switched)
	Wavelength	532 nm
	Output	450 mJ/pulse
Imaging system	Image tube	SIT tube
	Type	Hamamats photonics C1000-12 (superhigh-sensitivity camera)
Optical conditions	Resolution	2.5 mm (= $0 \sim 2\pi$)
	Inclination of sections	1.0°

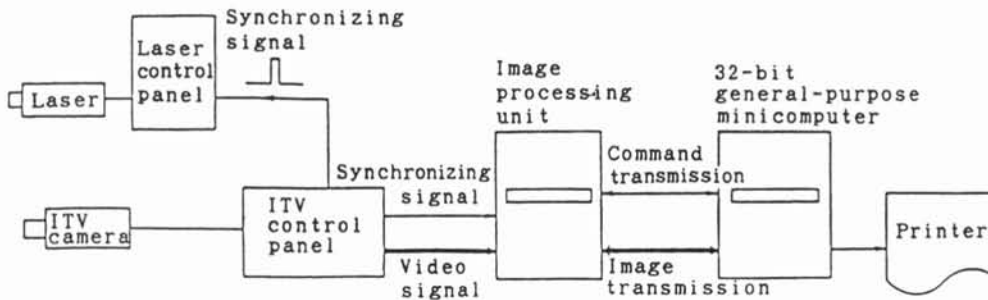


Fig. 4. Hardware configuration of image processing system.

4.2 Fourier transformation method

In the field of optical interferometric technology, Dr. Takeda of the University of Electro-Communications has devised the Fourier transformation method as a technique for obtaining high accuracy. We are pushing ahead with research to apply this principle to a plate flatness meter. The principle and application results of the Fourier transformation method are discussed below.

The light quantity distribution $g(x)$ of moire fringes that appear on the observation surface of an inclined moire fringe image is expressed by

$$g(X) = a(x) + b(x) \cos(2\pi f_0 x + 2\pi / \Delta z \cdot h(x)) \quad (4)$$

where,

$a(x), b(x)$ = spatial intensity distribution due to quantity difference in incident light or nonuniformity of reflectivity distribution on observation surface

$2\pi f_0 x$ = inclined component

Δz = contour line resolution

$h(x)$ = observation surface shape

For sake of convenience, the phase $\phi(X)$ is newly defined as follows:

$$\phi(X) \triangleq 2\pi / \Delta z \cdot h(x) \quad (5)$$

Equation (4) may be rewritten as follows:

$$g(X) = a(x) + b(x) \cos(2\pi f_0 x + \phi(X)) \quad (6)$$

The method of determining the phase $\phi(X)$ from Eq. (6) is considered as described below. If

$$c(X) \triangleq 1/2b(x) \cdot \exp(j\phi(X)) \quad (7)$$

then,

$$g(X) = a(x) + c(x) \exp(j2\pi f_0 x) + c^*(x) \exp(-j2\pi f_0 x) \quad (8)$$

where a complex conjugate is denoted by the

asterisk *. The Fourier transformation of Eq. (8) yields

$$G(\omega) = \int_{-\infty}^{\infty} g(x) \cdot \exp(-j\omega x) dx \quad (9)$$

$$= A(\omega) + C(\omega - 2\pi f) + C^*(\omega - 2\pi f)$$

where the large letters represent spatial frequency spectra concerning the variable x . Compared with the speed of change due to the carrier spatial frequency f , the change in $a(x)$ and $b(x)$ is very slow and so is the change in $\phi(X)$.

Therefore, the three spectra represented by Eq. (9) can be completely separated by the carrier frequency f .

The spectrum $c(\omega - 2\pi f_0)$ of signals on the positive carrier frequency f_0 is extracted and is shifted by f_0 toward the origin to obtain $C(\omega)$.

When $C(\omega)$ thus obtained is subjected to the inverse Fourier transformation with ω as the variable, $c(x)$ in Eq. (7) can be derived.

From,

$$\phi(X) = \tan^{-1} (\text{Im}[c(x)] / \text{Re}[c(x)]) \quad (10)$$

the disturbance term $b(x)$ can be separated and the phase $\phi(X)$ can be found.

The phase $\phi(X)$ of the moire fringe image shown in Fig. 3 and obtained by the Fourier transformation method is shown in Fig. 5. In Fig. 5, the dark portions denote 0 and the light portions denote 2π .

To determine the shape $h(x)$ from Eq. (5), the

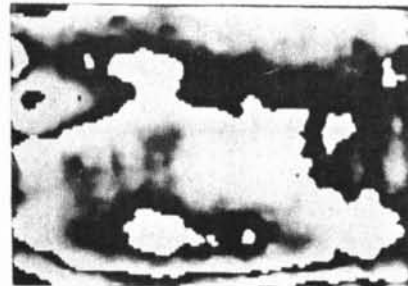


Fig. 5. Results of phase $\phi(X)$ calculation.

the phase $\phi(X)$ calculated by Eq. 10) must be compensated for the 2π jump. The shape $h(x)$ can be obtained directly by the 2π jump compensation.

The results of shape reconstruction are represented in terms of contour lines in Fig. 6.

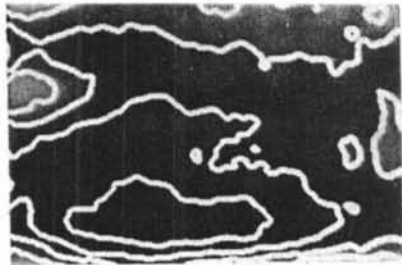


Fig. 6. Results of shape reconstruction (contour line representation).

4.3 Connection of shapes

The large grating is 2 m long and is not able to produce moire fringes of an entire plate at once. Therefore, longitudinal moire fringe images are lapped 0.5 m each and are introduced into the image processing unit. The shape of a portion of the plate is reconstructed from each image and the respective shapes are connected to obtain the whole-surface shape of the plate.

Ideally, the moire fringes at the trailing end of one image in the lap must coincide with those at the leading end of next image in the lap. In practice, however, the complete agreement of the moire fringes cannot be achieved, mainly due to the slight deformation the plate undergoes at it is transferred on the table.

The estimated shape of a portion of the plate in the lap is connected with that of the next portion of the plate in the lap that introduces a weight function as shown in Fig. 7:

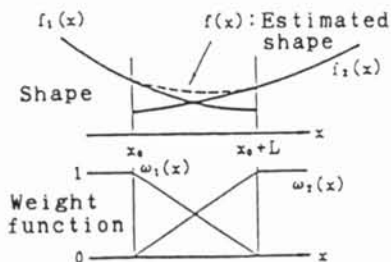


Fig. 7. Shape connection by weight function.

5. MEASUREMENT ACCURACY

A taut line was strung above and along the length of a plate. The shape of the plate was measured with a thickness gauge and was compared with the output of the flatness meter. The cross-sectional

shape of the plate is compared in Fig. 8, where the thickness gauge measurements are denoted by the open circles and the flatness meter output is represented by the solid line.

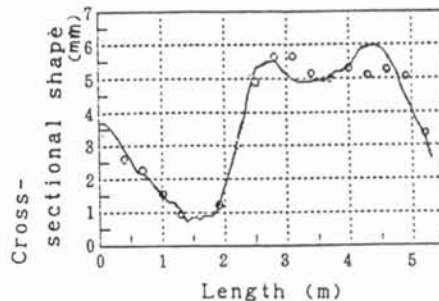


Fig. 8. Comparison of cross-sectional shape.

The overall measuring accuracy of the plate flatness meter is shown in Fig. 9. The number of flatness meter reading points that correspond to manual measuring points was $N = 204$ and the overall accuracy of $\epsilon = \pm 0.9$ mm (2σ) was achieved.

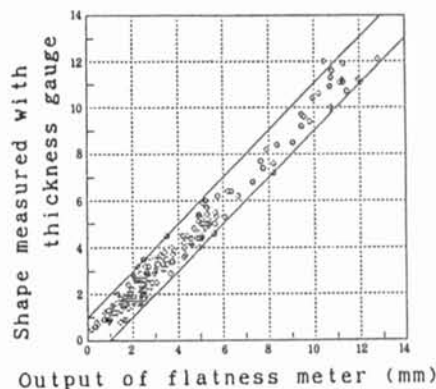


Fig. 9. Overall measuring accuracy

6. Acknowledgment

The authors gratefully thank Dr. Yatagai of the University of Tsukuba for guidance in the basics of image processing.

References

- (1) K. Kitamura et al.: "Development of hot steel shape measuring method based on laser moire method," *Tetsu-to-Hagane*, 68 (1982), p. s 1146.
- (2) H. Takasaki: "Moire Topography," *Appl. Opt.*, 9 (1970), p. 1457.
- (3) M. Takeda: "Fourier transform method of fringe pattern analysis for computer-based topography and interferometry," *J. Opt. Amer.*, 72 (1982), p. 156.